Physica Medica 146 (2026) 105811

Contents lists available at ScienceDirect

Physica Medica

journal homepage: www.elsevier.com/locate/ejmp

Original paper

Accounting for out-of-field dose and second cancer risk in classical Hodgkin lymphoma: A comprehensive comparison of proton and photon therapy using whole-body phantom

Mona Azizi [a,b,*], Maite Romero-Expósito [b,c], Forough Jafarian-Dehkordi [d], Isidora S. Muñoz-Hernández [e], Ignacio N. López-Martínez [e], Ignacio Espinoza [e], Ola Norrlid [f], Christina Goldkuhl [g], Daniel Molin [h], Beatriz Sánchez-Nieto [e], Iuliana Toma-Dasu [a,b], Alexandru Dasu [c,f]

[a] Stockholm University, Stockholm, Sweden
[b] Karolinska Institute, Stockholm, Sweden
[c] The Skandion Clinic, Uppsala, Sweden
[d] Otto von Guericke University, Magdeburg, Germany
[e] Institute of Physics, Pontificia Universidad Católica de Chile, Santiago, Chile
[f] Department of Immunology, Genetics and Pathology, Uppsala University, Uppsala, Sweden
[g] Sahlgrenska University Hospital, Gothenburg, Sweden
[h] Uppsala University, Uppsala, Sweden

ARTICLE INFO

Keywords:
Hodgkin lymphoma
Out-of-field dose
Proton therapy
VMAT
Integral dose
Risk assessment

ABSTRACT

Background: Although out-of-field radiation doses are lower than in-field doses, they may still contribute to late toxicities and second cancer risk in classical Hodgkin lymphoma (cHL) patients. Moreover, treatment planning systems (TPS) often underestimate these doses, especially in healthy tissues.

Methods: Dosimetric parameters were compared between pencil beam scanning proton therapy (PBS) and volumetric modulated arc therapy (VMAT) in a cohort of 20 patients from the PRO-Hodgkin study. Planning CT scans were reconstructed into virtual whole-body CTs using the IS^{2}aR software. Out-of-field doses were estimated with analytical models and Monte Carlo simulations in whole-body phantoms, then integrated with TPS in-field doses to calculate total equivalent dose. Dose distributions, dose–volume histograms (DVHs), non-target tissue integral dose equivalent (*NTIHs*), mean organ doses, and lifetime attributable risks of Second cancer (*LARs*) were evaluated for critical healthy tissues.

Results: PBS consistently resulted in lower out-of-field doses than VMAT. In both modalities, contributions were relatively small, not exceeding 5% of the prescribed dose. For organs near the target such as thyroid, lungs, breasts, heart, and esophagus, mean dose differences between PBS and VMAT ranged from 1.3 to 4.5 Sv, while for distant organs differences remained below 0.3 Sv. Incorporating out-of-field doses into *LAR* estimates increased predicted risks, but PBS reduced these values by up to 40% compared to VMAT.

Conclusion: The radiation burden in high-precision radiotherapy, particularly from out-of-field radiation, should be accounted for in epidemiological studies and incorporated into treatment planning optimization to minimize second cancer risks in cHL patients.

1. Introduction

Radiation therapy (RT) is successfully used in the treatment of stage I and II classical Hodgkin lymphoma (cHL) [1]. The majority of patients achieve long-term survival after their treatment, but they remain susceptible to health complications including cardiovascular and pulmonary issues as well as second malignancies [2,3]. Strategies to minimize the risk for these effects include using advanced RT techniques which minimize the exposure of the normal tissues complemented by regular long-term follow-up [1–3]. Most experience from radiation

* Corresponding author at: Cancercentrum Karolinska (CCK), Karolinska Sjukhuset i Solna, Visionsgatan 56A, våning 3, 171 76 Stockholm, Sweden.
E-mail address: mona.azizi@fysik.su.se (M. Azizi).

https://doi.org/10.1016/j.ejmp.2026.105811
Received 3 October 2025; Received in revised form 17 March 2026; Accepted 23 April 2026
Available online 2 May 2026

induced second malignancies is from studies following total body exposure to low absorbed doses of ionizing radiation, much lower than those typically administered in RT [4,5]. Consequently, the International Commission on Radiation Units and Measurements (ICRU) Report No. 83 [2] recommended accounting for the dose to the volume of the patient's body excluding the target and the organs-of-interest (OOI), in the evaluation of the treatment plan.

Compared to three-dimensional conformal radiotherapy (3D-CRT), modern techniques such as IMRT and VMAT provide superior target conformity and sparing of critical structures but at the cost of exposing a larger volume of healthy tissues to low or very low doses, potentially increasing second cancer risk [6–11]. While optimized VMAT can reduce high-dose exposure to the heart relative to IMRT, it may increase low-dose exposure to the lungs, which could also elevate the probability of inducing a second cancer [12].

Proton therapy (PT) is a treatment technique that can deliver dose distributions with improved target conformity and better sparing of OOIs due to the distinctive dose deposition pattern of protons, characterized by the Bragg peak with reduced entrance exposure and steep fall-off at the end of the particle range. Consequently, PT can reduce low-intermediate doses outside the target volume compared to VMAT and IMRT [4]. Thus, PT has potential to reduce late-onset toxicities in cardiac, pulmonary, esophageal, and thyroid tissues and to lower the risk of second cancers [12–15]. However, PT is characterized by a mixed radiation field of particles with a non-negligible production of secondary neutrons compared to photon RT [16–18]. Indeed, interaction of the protons in the beam line and the patient leads to the generation of secondary neutrons that can travel farther away from the target volume (TV) compared to the primary radiation that is confined around the TV. Neutrons, produced as long-range secondary particles in PT, contribute to doses in the low-dose range and can thus affect organs far from the TV [5]. Understanding the impact of the secondary radiation on the risk of radiation-induced second cancers is therefore essential for the assessment of risks from modern RT techniques [19,20].

Modern RT is highly individualized, with treatment plans optimized for the individual characteristics of each patient [21]. Favorable beam arrangement and optimization strategies can lead to substantial reductions in PBS compared to VMAT in V_{20} (the volume of an organ receiving at least 20 Gy) and V_{30} (the volume of an organ receiving at least 30 Gy) for the breasts, lungs, heart, and spinal cord [12,22,23]. This is particularly relevant for patients with mediastinal cHL, given the proximity of their target to important thoracic structures such as the breasts, heart, and lungs. While dose optimization is mainly done from the perspective of primary doses, the impact of scattered and secondary radiation is less explored.

Furthermore, while modern RT techniques such as VMAT and IMRT have significant clinical benefits, they are suspected of increased radiation exposure to low doses due to the high amount of monitor units (MUs), that could lead to two to three times more leakage radiation to the patient's body [24]. Likewise, these techniques can expose larger volumes of non-target tissues to low-dose radiation, thereby increasing the integral dose [25]. It is generally accepted that the non-target integral dose can enhance normal tissue toxicities and the risk of second malignancies, however, it is still not commonly used in clinical practice for comparing treatment plans or evaluating outcomes [26]. To date, no clear threshold has been established for determining what level of non-target integral dose increase can be regarded as acceptable in clinical practice. Nonetheless, in line with best practice and with the As Low As Reasonably Achievable (ALARA principle), it is recommended to minimize the integral dose while maintaining the target coverage in order to limit the exposure of healthy tissues to ionizing radiation [27].

To address this knowledge gap, this study aimed to conduct a comparative dosimetric analysis of patients with classical cHL treated with PT with pencil beam scanning (PBS) and with photon-based VMAT. The analysis focused on the out-of-field doses calculated from each patient's individual treatment planning data in addition to the doses to the target and the healthy organs. The study also assessed the risk of second cancer associated with the total equivalent dose in both PBS and VMAT techniques.

2. Materials and methods

2.1. Patient cohort and treatment planning

Twenty patients with cHL with mediastinum and/or neck involvement were included in this study. All patients were treated within the PRO-Hodgkin study (ClinicalTrials.gov ID: NCT06883604). The cohort comprised 6 females and 14 males, aged 19 to 53 years, with lymphoma in the mediastinal area and some of them with involvement of the neck or axilla areas. The patients received PT at the Skandion Clinic in Uppsala, Sweden, using the PBS delivery system ProteusPlus from IBA (Ion Beam Applications, Louvain-La-Neuve, Belgium), with energies ranging from 60 to 180 MeV depending on the target location. For the PBS modality, plans were made using the Eclipse treatment planning system (TPS) (Varian Medical Systems, Palo Alto, USA). A photon VMAT plan was also made for each patient as part of their selection for PT. The VMAT treatment plans were made using the Monaco TPS (Elekta AB, Stockholm, Sweden) according to the guidelines at the Uppsala University Hospital, Uppsala, Sweden [28,29]. The prescribed equivalent dose to the target volume was classified into two groups according to the presence of clinical risk factors: a high-dose group receiving 29.75 Gy (RBE) in 17 fractions, and a low-dose group receiving 20 Gy (RBE) in 10 fractions, for both photon and proton plans. The same contours for the clinical target volume (CTV) and OOIs were used for both the PBS and VMAT plans. A standard CTV-to-PTV margin of 5 mm for low-dose and 7 mm for high-dose groups was used for the VMAT plans, while the proton plans were robustly optimized based on CTV using 4.5% range uncertainty and 5–7 mm setup uncertainty depending on target size and localization. For both plans, optimization was performed in accordance to the International Lymphoma Radiation Oncology Group (ILROG) guidelines [28,29].

2.2. Assessment of the total dose including the out-of-field doses

The assessment of the total absorbed dose is generally possible for organs in the scanned volume used for treatment planning, however this is a challenge for organs situated outside the planning CT volume. The lack of information in the planning CT about the patient anatomy outside the scanned volume could be supplemented through the use of whole-body computational phantoms that provide detailed anatomy of out-of-scan organs and enabling three-dimensional dose calculations for tissues outside the TV [19]. For this purpose, a modified version of MATLAB-based Interactive Software for Image Segmentation and Registration (IS^2aR) [19,30] was employed in the present investigation. The software generates a whole-body CT for individual patients by combining their planning CT with an appropriately-modified reference phantom from ICRP-110 [31]. For the organs for which contours were not available from the TPS, the contouring tools from the automatic segmentation tool Total Segmentator were used to generate the corresponding delineations [32].

Another challenge in estimating the total dose received during the RT is the limited information on the secondary radiation contribution. TPSs often underestimate the dose delivered to organs located far from the primary target [33]. To overcome this issue for the VMAT plans of the present study, only photon absorbed dose distributions within the 5% isodose volume were extracted directly from the TPS. For regions outside the 5% isodose, photon secondary doses were estimated using the Periphocal 3D (P3D) software [34]. The Periphocal 3D model was based on Monte Carlo (MC) simulations of peripheral dose for a 6 MV treatment using the ICRP-110 phantom and validated with thermoluminescent dosimeter measurements in an ATOM phantom under VMAT irradiation. This software calculates the 3D out-of-field dose distribution

in the whole-body phantom model of each patient based on input parameters such as the prescribed dose, monitor units, the mean field size (defined by the 50% isodose), isocenter location, and CT of the patient which have been extracted from each individual VMAT plan. The output is a total whole-body dose matrix containing all structures presented in the ICRP-110 produced by IS^{2}aR.

For the proton plans, the contribution of secondary neutrons was assessed by MC simulation. The modeling of the proton beam at Skandion Clinic has been described previously using the MCNP 6.2 code [35–37]. The MCNP default configuration was used, consisting of the ENDF nuclear data library and the Cascade-Exciton Model (CEM) for high-energy nuclear interactions [37]. The proton source was defined at the nozzle exit and, therefore, only internally generated secondary neutrons (with the additional contribution of the range shifter when used in the plan) were considered. Each patient plan was simulated reproducing the clinical treatment plan layer by layer, accurately modeling the distribution of proton spots. As with photon plans, a voxel-by-voxel approach was followed. The neutron dose equivalent in each voxel for each whole-body phantom was computed, taking into account the energy dependence of the radiation quality factor (Q) for neutrons [38,39]. The evaluation of dose equivalent following this approach introduces additional uncertainties associated with the use of those factors. Experimental studies assume uncertainties not lower to 20% to this approach [4,40]. Further uncertainties arise from the data libraries and nuclear models used in the simulations to score the neutron energy distributions. Comparisons between different Monte Carlo codes using default settings have shown differences of up to 16% in the dose equivalent due to spectral differences [41]. With these considerations in mind, the number of primary protons simulated was chosen as a compromise between reasonable computation time and reduced statistical uncertainty, targeting values below 10%. Depending on the patient, the number of simulated primary protons ranged from 8×10^8 to 1.5×10^9. Finally, the total dose matrix was obtained summing the neutron dose equivalent distribution to the proton dose equivalent distribution extracted from the TPS. For consistency, the proton absorbed dose was weighted using a different RBE/weighting factor depending on the region [19]. The usual clinical RBE of 1.1 was applied to the in-field dose (inside the 50% isodose), while a w_R of 2 was applied to the out-of-field dose, following the proposal by Romero-Expósito et al. [19]. As a result, the dose distributions will be expressed in units of dose equivalent, Sievert (Sv). The assumption that Gy (RBE) is equivalent to the Sievert was made only in the in-field area. However, this will not have an impact on the estimated risk of second cancer in the patient's organs.

2.3. Evaluation of the non-target integral dose equivalent

The integral dose, indicating the total energy deposited in the healthy tissue gives a measure for healthy organ sparing, with a lower integral dose indicating reduced exposure to healthy tissues. In this study, we evaluated a modified metric focusing exclusively on non-target tissues denoted as a non-target tissue integral dose equivalent (*NTIH*). The *NTIH* was defined as the volume-averaged dose equivalent to all voxels outside the target volumes and was calculated as:

$$NTIH = \frac{1}{V_{NT}} \sum_{i=1}^{m} H_i V_i$$

Here, H_i and V_i represent the dose equivalent and volume of voxel i, respectively, while V_{NT} denotes the total volume of the non-target tissue. The summation is performed over all voxels i belonging to non-target tissues, with all target volume voxels excluded. As all voxels in a given patient dataset have identical volume, this formulation corresponds to a volume-averaged dose equivalent in non-target tissues. The *NTIH* was derived from the 3D total dose equivalent distributions, explicitly accounting for the out-of-field doses for both the proton and photon plans.

2.4. Evaluation of lifetime attributable risk including the out-of-field doses

The lifetime attributable risk of second cancer (*LAR)* for both PBS and VMAT treatment plans was estimated accounting for the total dose equivalent delivered. Dose-volume histograms (DVHs) were generated for the different organs across all patients. In both treatment modalities, the DVHs accounted for the contributions of the primary and secondary radiation and an equivalent dose was calculated taking into account the type of radiation contributing to the total equivalent dose [19]. The *LAR* values were calculated for each patient, accounting for their age at exposure, with an assumed attained age of 70 years and a latency period of 5 years.

The dose–response relationship between radiation exposure and in vivo cancer risk is complex and remains an area of active investigation [43,44]. According to AAPM Report No. 158, cancer risk increases approximately linearly with dose up to about 2 Sv [45], whereas at higher doses the dose–response relationship becomes more uncertain, and additional biological effects, such as cell killing, may influence risk estimates [46]. For organs receiving doses below 2 Sv, cancer risk can be estimated using linear no-threshold models, such as those proposed by BEIR [42] or ICRP [37], which rely on the mean dose. In contrast, for dose levels exceeding 2 Sv [19], risk assessment models typically incorporate dose distributions or voxel-level calculations [18]. In this study, two risk models were applied according to the organ-equivalent dose. For equivalent doses greater than 2 Sv, the Schneider mechanistic model, accounting for cell killing and fractionation effects, was used through the organ equivalent dose (OED) formalism [19]. Conversely, the BEIR VII linear no-threshold model was applied for equivalent doses below 2 Sv [42].

3. Results

3.1. Dose analysis accounting for out-of-field doses

The dose equivalent distributions from the PBS and VMAT plans for one individual patient (#7 in the patient cohort) which was prescribed 29.75 Gy (RBE) in 17 fractions is presented in Fig. 1. This patient is in the middle range of doses in the cohort, hence the suitable choice for the illustration of the difference between the dose distribution rendered by the TPS, confined to planning CT area, and the calculated total equivalent dose accounting for the contribution of out-of-field doses covering the whole-body phantom.

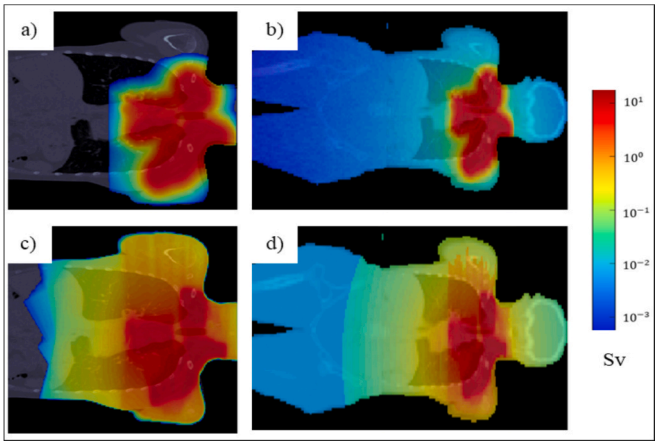

Fig. 1. Comparison of dose equivalent distributions in photon and proton plans for a representative cHL patient (#7) from the high-dose group a) primary proton dose distribution from the TPS for the PBS plan; b) total dose equivalent in the whole-body CT for the proton plan; c) primary photon dose from the TPS for the VMAT plan; and d) total dose equivalent in the whole-body phantom for the VMAT plan. Please note that the dose scale is logarithmic.

Fig. 2 presents the DVHs for the esophagus, comparing the primary dose from the TPS with the total equivalent dose, which includes secondary dose contributions, for both proton and photon plan to illustrate the importance of accounting for the total equivalent dose with respect to the volume receiving very low doses. The inserts display the low-dose regions below 0.1 Sv, where the contribution from neutron radiation becomes evident in the proton plan in Fig. 2a. The total equivalent dose in the photon plan includes primary radiation and the estimated low-dose contributions from scattered radiation, observed at below 1.4 Sv outside the 5% isodose region. The total equivalent dose shows that including scattered radiation shifts the photon plan curve upward, indicating higher volumes and highlighting that the TPS may underestimate secondary doses when out-of-field contributions are excluded. Although the esophagus was selected to illustrate the impact of secondary radiation, it should be noted that secondary radiation doses may be even higher in relative terms, for organs located farther from the TV, where the contribution from stray radiation becomes more prominent compared to the primary dose.

Table 1 presents the equivalent neutron and total equivalent doses in the PBS plan, along with the secondary and total photon doses in the VMAT plan for the representative patient #7. For PBS plans, the reported equivalent dose includes contributions from both primary protons and secondary neutrons. For VMAT plans, the equivalent dose accounts for photon contributions from primary and secondary radiation. Organs located closer to the TV receive higher neutron doses than those farther away. The thyroid received the highest neutron dose of 90 mSv, followed by the spinal cord at 70 mSv and the esophagus at 66 mSv. The uterus and ovaries received some of the lowest neutron doses, each at 2 mSv.

In the PBS plan, total equivalent dose ranges from 2 mSv to 20.3 Sv across different organs. The thyroid receives the highest dose at 20.3 Sv, followed by the esophagus at 9.5 Sv. Due to the tumor's location on the left side, the left lung received 6.0 Sv, while the right lung received 3.1 Sv. Moreover, the neutron equivalent dose was 34% higher in the left lung than in the right one. Similarly, the dose received by the left breast was 0.6 Sv, which was ten times higher than that received by the right breast. Distant organs like the liver, stomach, spleen, uterus, and ovaries received no primary proton dose, and despite increased neutron contributions, total doses remained minimal. Neutron dose equivalent in organ was generally obtained with statistical uncertainties below 10%. For organs in the head, thorax, and abdomen, the uncertainties were below 5%.

In the VMAT plan, total equivalent doses vary between 8.0 Sv to 19.0 Sv across different organs. The thyroid, situated within a high-dose region, receives the highest dose at 19.0 Sv. Among the organs, the lungs experience the most significant contribution from secondary radiation, with each receiving nearly 0.4 Sv to a total equivalent dose of 7.0 Sv for the left lung and 3.6 Sv for the right. In contrast, organs located in low-dose regions, such as the liver, stomach, spleen, uterus, and ovaries, are only affected by secondary radiation, and the total equivalent doses in these organs remain below 0.2 Sv.

The comparison of total equivalent doses between PBS and VMAT for the representative patient revealed notable differences across organs. PBS consistently resulted in lower doses to healthy tissues, except for the

Table 1
Equivalent doses in selected organs for a representative cHL patient (#7) from the high-dose group, using both PBS and VMAT techniques. In the PBS plan, the total dose includes both the proton and neutron contributions, while in the VMAT plan, it consists of the photon dose contributions from both the primary and secondary radiation.

Organs	Equivalent dose for 17 fractions (mSv)				Ratio of total equivalent dose (VMAT/PBS)
	PBS plan		**VMAT plan**		
	Neutrons	**Total**	**Secondary radiation**	**Total**	
Thyroid	9.0×10^1	20.3×10^3	–	19.0×10^3	0.9
Esophagus	6.6×10^1	9.5×10^3	2.0×10^2	11.2×10^3	1.2
Left Lung	4.8×10^1	6.0×10^3	3.5×10^2	7.0×10^3	1.2
Right Lung	3.2×10^1	3.1×10^3	4.0×10^2	3.6×10^3	1.2
Spinal cord	7.0×10^1	4.0×10^3	0.7×10^1	13.1×10^3	3.3
Left Breast	2.7×10^1	6.0×10^2	1.8×10^2	1.0×10^3	2.0
Right Breast	1.7×10^1	6.1×10^1	2.3×10^2	1.4×10^3	25.0
Heart	3.0×10^1	6.3×10^2	3.6×10^2	1.0×10^3	1.6
Liver	1.0×10^1	1.0×10^1	2.0×10^2	0.2×10^3	20.0
Stomach	1.0×10^1	1.0×10^1	1.8×10^2	0.1×10^3	10.0
Spleen	1.0×10^1	1.0×10^1	1.5×10^2	0.1×10^3	10.0
Uterus	0.2×10^1	0.2×10^1	0.8×10^1	0.8×10^1	4.0
Ovaries	0.2×10^1	0.2×10^1	0.8×10^1	0.8×10^1	4.0

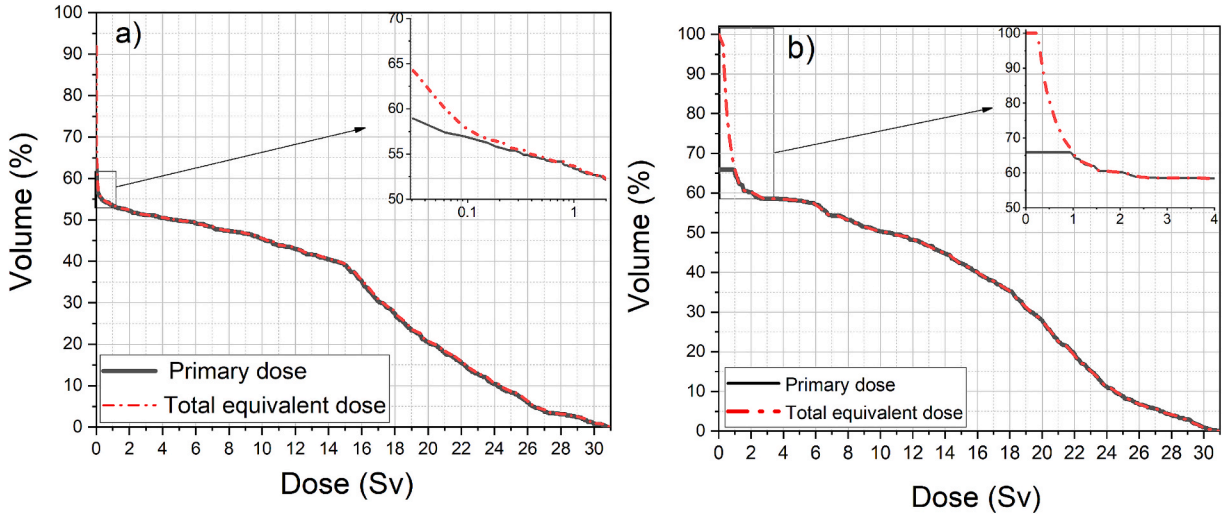

Fig. 2. DVH for the esophagus, for a) the primary and total equivalent dose for the proton plan and b) the same for the photon plan for cHL patient #7.

thyroid located within the target volume. For example, VMAT delivered 25 times more total equivalent dose to the right breast and 20 times more to the liver compared to PBS. The VMAT-to-PBS total equivalent dose ratio ranged from 1.2 to 25. These findings underscore the advantage of PBS in sparing healthy tissue, while VMAT's broader dose distribution calls for careful planning to minimize toxicity.

3.2. Dosimetric comparison of total equivalent doses in the patient cohort

Fig. 3 compares the mean organ doses from the total proton and photon plans in the cohort of 20 cHL patients. The total proton plan consistently resulted in lower mean doses across all organs. Doses ranged from < 0.1 mSv to 13.2 Sv to in the total proton plan and from 5 mSv to 15.5 Sv in the total photon plan. For organs close to the TV, such as the thyroid, lungs, breasts, heart, and esophagus, the mean dose differences ranged from 1.3 to 4.5 Sv. Moreover, reductions of 38%, 48%, 50%, and 61% were observed in the right lung, left lung, left breast, and right breast, respectively. For organs located farther from the target, including the stomach, liver, bladder, colon, and prostate, dose differences were under 0.3 Sv.

Fig. 4 illustrates the *NTIH* values for the total proton and total photon dose distributions across all treatment fractions for the 20 patients. Patients 1–14 were in the high-dose prescription group, while the remaining (15–20) were in the low-dose prescription group. As noted above, the total photon and proton plans represent the dose equivalent distributions accounting for the out-of-field doses in both modalities, including secondary dose contributions. As expected, the results show that the *NTIH* of the proton plans is consistently lower than that of the corresponding photon plans. The patient-specific *NTIH* values for the total photon and proton plans range from about 0.2 to 2.2 Sv and 0.1 to 1.3 Sv, respectively.

Despite both plans being designed to achieve equivalent target coverage and healthy organ sparing, the *NTIH* values are significantly higher in all total photon plans than in the total proton plans. The highest and lowest photon-to-proton *NTIH* ratios are 2.8 and 1.2, respectively, found in two patients (#2 and #14 in Fig. 4) from the high-dose group. The high *NTIH* values in total photon plans suggest that larger volumes of organs close to the TV are exposed to a low-dose radiation bath compared with total proton plans. In VMAT, these low-dose volumes arise from machine scatter and leakage, yielding increased integral doses to the organs outside the TV.

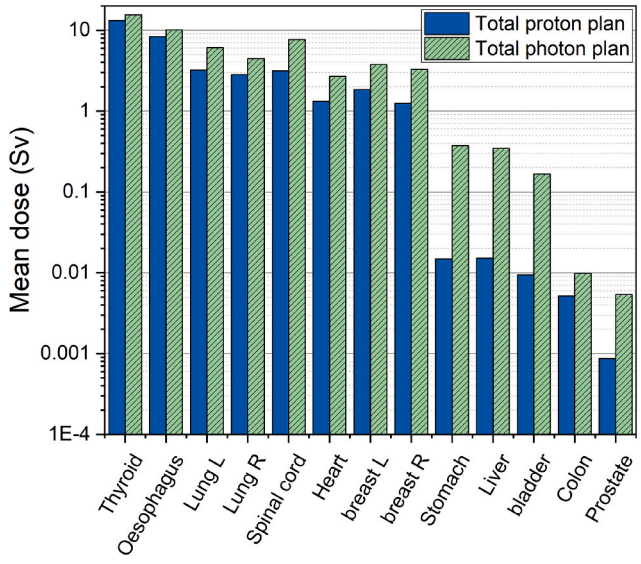

Fig. 3. Comparison of mean doses (Sv) to the organs from the total proton and photon plan across 20 patients with cHL.

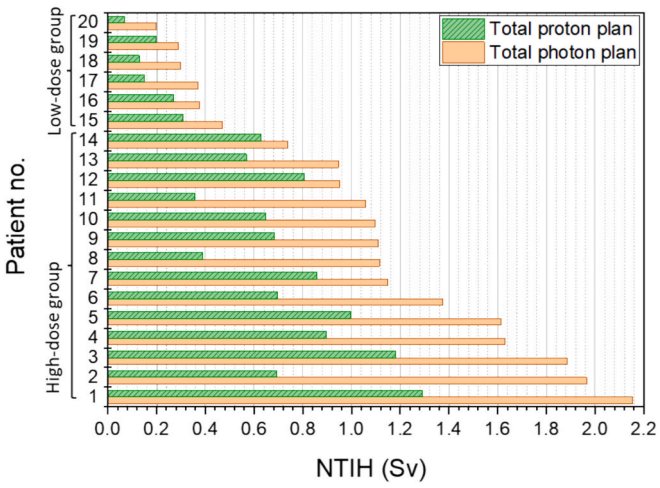

Fig. 4. Non-target integral dose equivalent (*NTIH*) (Sv) for the total proton and photon plan across all treatment fractions in 20 cHL patients.

3.3. Estimating lifetime attributable risk accounting for the out-of-field doses

The *LAR* (%) estimated for the development of lung cancer induced by RT from both the total dose and primary plan in PBS and VMAT plans for 20 cHL patients are depicted in Fig. 5. Patients 1–14 were assigned to the high-dose group, while the remaining (15–20) were assigned to the low-dose group. The *LAR* (%) values were derived using the Schneider or BEIR risk models, based on the equivalent dose to specific organs. Fig. 5 illustrated that the *LAR* (%) for the total photon plan is higher than that for the total proton plan, ranging from 4.7% to 2% in the high-dose group and from 1.9% to 0.3% in the low-dose group, compared to 3.2% to 1% and 1.1% to 0.1% for the proton plan, respectively.

In terms of the effect of secondary radiation on the risk of radiation-induced lung malignancies from PBS and VMAT plan, Fig. 5 shows that the *LAR* (%) from both the total proton and photon plan is higher compared to their respective primary plan. Among individual cHL patients, the difference between maximum and minimum *LAR* (%) in the

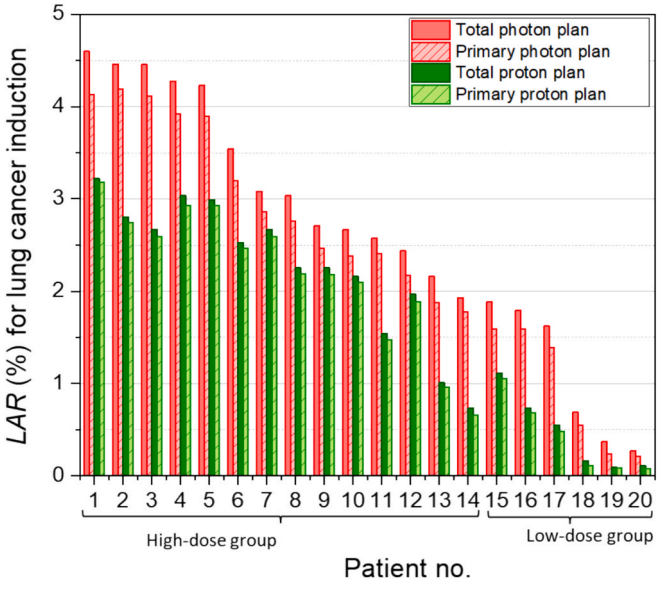

Fig. 5. Comparison of lifetime attributable risk (*LAR* (%)) for lung cancer induction for 20 cHL patients assuming the dose distribution in the total photon plan, primary photon plan, total proton plan, and primary proton plan, respectively.

total versus primary photon plans ranges from 0.1% (#20 in Fig. 5) to 0.5% (#1 in Fig. 5). This variation is associated with the low-dose radiation, which is not accounted for in the primary photon plan. A similar trend is observed in the proton plan, with a maximum *LAR* (%) difference of 0.2% (#4 in Fig. 5), due to the TPS's limitations in accurately calculating secondary neutron production during proton therapy.

Fig. 6 shows the *LAR* (%) values for various organs, including the thyroid, lungs, esophagus, female breasts, stomach, liver, bladder, colon, uterus, and ovaries in female patients, as well as the prostate in male patients, across the 20 cHL cases for both total photon and proton plan after accounting for all contributing secondary radiation doses. For the total photon plan, the overall *LAR* (%) ranged from 3.5% to 7.7% in the high-dose group and from 1.3% to 3.3% in the low-dose group. For the total proton plan, the corresponding ranges are 3.4% to 5.3% and 0.5% to 3.8%. The largest *LAR* (%) difference between the two total proton and photon plan is observed in one patient (#8 in Fig. 6) from high-dose group, with values of 1.8% and 5.2%, respectively.

Overall, the highest *LAR* (%) values were observed in the lungs, thyroid, and female breasts. As the thyroid is typically located within the treatment field in most cHL cases, comparable *LAR* (%) values were observed between the total photon and proton plans, ranging from 0.1% to 2.1%. For instance, patient #1 exhibited identical thyroid *LAR*s of 2.1% for both modalities, while patient #2 demonstrated the highest discrepancy between the two, with a difference of 1.1%.

Although the *LAR* (%) values for the lungs are lower in the total proton plan compared to the total photon plan, the lungs still show the highest *LAR* (%) overall, with values ranging from 0.1% to 4.4% in the total photon plan and 0.1% to 3.0% in the total proton plan. A similar trend is observed for the female breasts, where *LAR* (%) values range from 0.3% to 2.2% in the total photon plan and from 0.1% to 1.7% in the total proton plan. The reproductive organs have the lowest values (below 0.1%). For the remaining organs located far from the treatment area, the *LAR* (%) values remain below 1% in all patients for both modalities.

3.4. *LAR (%) versus NTIH*

Fig. 7 presents a scatter plot showing the ratio of *NTIH* for the total proton plan to the total photon plan on the x-axis, plotted against the corresponding ratio of *LAR* for the total proton plan to the total photon plan on the y-axis, for cHL patients. The red stars in the Fig. 7 are representative of the low-dose group. As most radiosensitive organs such as the lung and breast are located further from the TV, all the patients in the low-dose group lie below the identity line, indicating lower *LAR* ratios compared to the *NTIH*.

Across all patients, the *NTIH* delivered by total proton plan is consistently lower than the total photon plan, with all *NTIH* ratios falling below 1.0. These ratios span approximately from 0.3 and 0.7, indicating that the total proton plan reduces the dose to non-target tissues nearly by 30% to 70% compared to the total photon plan. Similarly, the *LAR* ratios also lie below 1.0, ranging from approximately 0.3 to 0.9, corresponding to a 10% to 70% reduction relative to the total photon plan. Some patients with similar *NTIH* ratios of approximately 0.6, had varying *LAR* ratios of 0.5 (#2 in Fig. 6), 0.7 (#6 in Fig. 6), and 0.8 (#7 in Fig. 6), indicating a high increase in estimated risk.

Fig. 8 shows the variation in *LAR* (%) as a function of attained age (40–100 years) for three cases: lung and breast cancer risks in a 21-year-old female patient (#3 in Fig. 6) with OEDs of 3.0 Sv and 2.6 Sv, respectively, and lung cancer risk in a 19-year-old male patient (#8 in

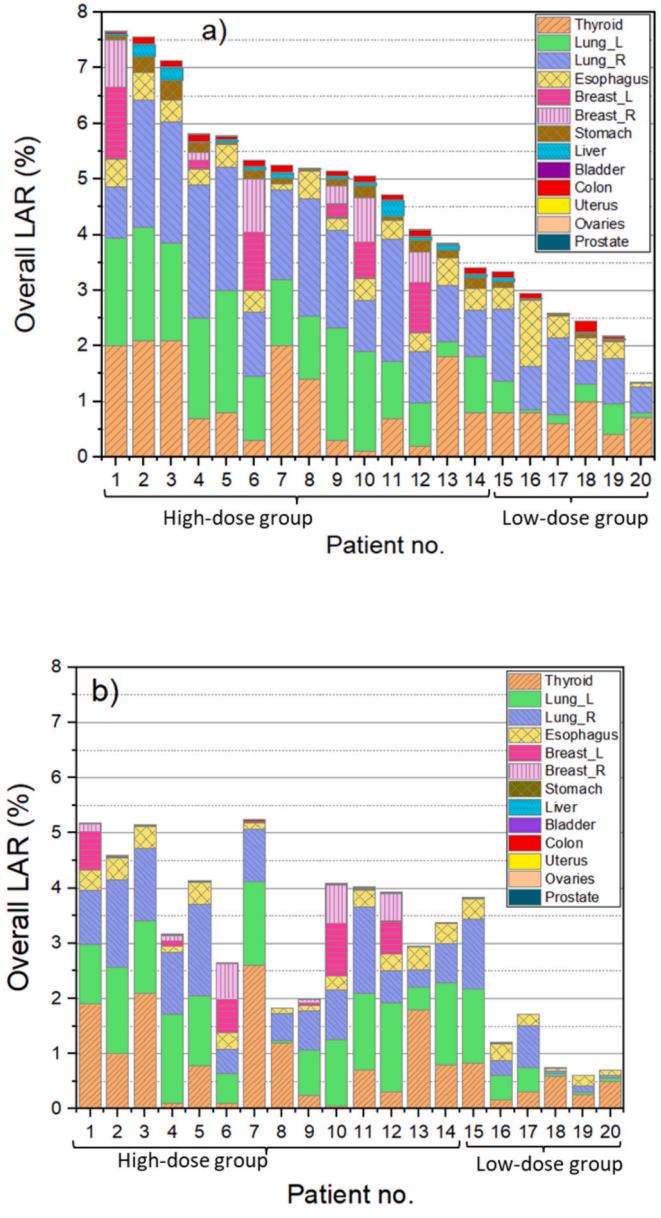

Fig. 6. Comparison of organ-specific overall lifetime attributable risk (*LAR*) (%) between a) the total photon plan and b) the total proton plan in 20 patients with cHL.

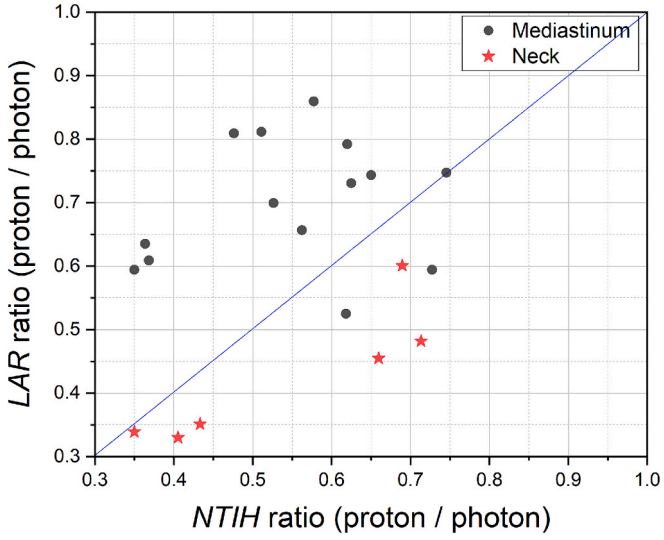

Fig. 7. Scatter plot of the ratio of modified non-target integral dose equivalent (*NTIH*) for the total proton plan to the total photon plan versus the ratio of lifetime attributable risk (*LAR*) for the total proton plan to the total photon plan for 20 cHL patients.

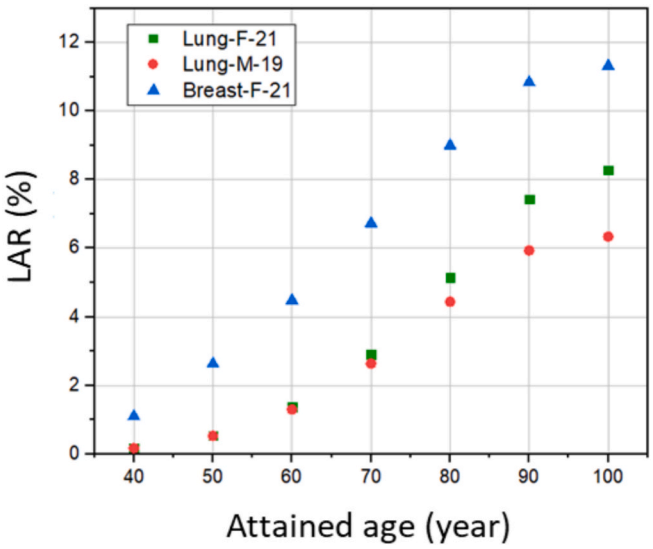

Fig. 8. *LAR* (%) as a function of attained age for three cases: lung cancer risk in a 21-year-old female with OED of 3 Sv (green), breast cancer risk in the same female with OED of 2.6 Sv (blue), and lung cancer risk in a 19-year-old male (red). (For interpretation of the references to colour in this figure legend, the reader is referred to the web version of this article.)

Fig. 6) with an OED of 3.1 Sv.

An increasing trend in the *LAR* (%) with attained age is observed for all cases. For instance, in the 21-year-old female, the *LAR* (%) for lung increased from approximately 0.2% at an attained age of 40 years to 8.2% at 100 years. A similar trend was seen in the 19-year-old male, though with consistently lower *LAR* (%) values from 0.2% to 6.3%. This is consistent with the cumulative nature of radiation-induced cancer risk, where longer survival allows more time for a potential malignancy to develop.

Sex-specific differences are also evident. Despite similar ages at exposure and identical OEDs, the female patient showed higher *LAR* (%) values for lung cancer than the male patient at all attained ages. At age 80, for example, the *LAR* (%) for the male lung was 4.5%, compared to 5.2% in the female.

Furthermore, the comparison of organ-specific radiosensitivity in the female patient showed substantial differences. The *LAR* (%) for breast cancer was consistently higher than for lung cancer at all attained ages. At age 50, the *LAR* (%) was 2.5% for breast and 0.9% for lung, increasing to 6.8% for breast and 3% for lung at age of 70, and reaching 9.1% for breast and 5.3% for lung at age 80. Breast *LAR* consistently exceeds lung *LAR*, with a steeper slope (~0.18% vs. ~0.13% per year), highlighting greater breast radiosensitivity. Although Fig. 8 presents results for two representative patients, the observed trends are consistent across the cHL patient cohort and therefore the conclusions drawn are representative for the overall study population.

4. Discussion

In this study, dosimetric parameters were compared between PBS and VMAT plans in 20 patients from the PRO-Hodgkin study treated for cHL. The aim was to evaluate the total radiation dose delivered to the TV and surrounding healthy tissues by incorporating analytically-estimated out-of-field doses. To enable a comprehensive and patient-specific assessment, we applied a previously developed methodology that integrates out-of-field and in-field doses calculated by the TPS, providing a more accurate comparison of overall radiation exposure between the two modalities [19].

To the best of our knowledge, this is the first study to compare PBS and VMAT in a cHL cohort with a specific focus on out-of-field radiation dose. When comparing PBS and VMAT in terms of healthy-organ sparing, our results showed notable differences in mean dose for organs located near or partially within the TV (Fig. 3). Specifically, dose reductions with PBS compared to VMAT reached up to 1.8 Sv for the esophagus, 2.0 Sv for the female breast, 2.3 Sv for the thyroid, 2.8 Sv for the lungs, and 4.0 Sv for the spinal cord. In contrast, for organs located farther from the TV, the dose differences between the two modalities were consistently below 0.5 Sv. Nonetheless, our findings are in agreement with previous investigations that have reported significant reductions in dose to healthy organs when PT is compared to conventional photon-based techniques. These studies consistently highlight the dosimetric advantages of PT, particularly its potential to reduce radiation exposure to healthy tissues located outside the TV [44,47–53].

As emphasized in AAPM TG-158, out-of-field radiation doses, though lower than in-field doses, can be clinically relevant and are often underestimated by TPS, warranting their inclusion in total dose assessments [16]. In line with this, our analysis demonstrates that incorporating out-of-field doses leads to higher estimates of the total equivalent dose compared to those derived solely from TPS data (Table 1). In our representative patient, the highest mean out-of-field doses were observed in the thyroid and right lung, and were due to neutrons and secondary photons, respectively. These doses corresponded to 0.3% and 1.4% of the prescribed dose in the total proton and photon plans. As previously noted, this representative patient is positioned near the median of the cHL cohort; therefore, higher out-of-field dose values may be observed in some cases. Nevertheless, across all patients and in both treatment modalities, the out-of-field doses consistently remained below 5% of the prescribed dose.

A strength of this study is the use of a synthetic whole-body imaging for each individual patient, allowing for more accurate estimation of radiation doses to distant organs outside the primary treatment fields. Various methods exist to construct whole-body anatomical models, such as employing computational phantoms or generating synthetic representations [54–56]. This study adopted the IS^{2}aR framework that generates patient-specific anatomical geometries using each individual's planning CT. Furthermore, two RBE models were applied to the PT plans to improve the assessment of the biologically equivalent dose and second cancer risk, with a particular emphasis on out-of-field regions. While clinical PT typically assumes a constant RBE of 1.1, studies have shown that RBE values can increase up to approximately 2 near the distal edge of the Bragg peak due to elevated linear energy transfer (LET) [57,58], as well as in regions receiving very low doses. The interest in variable RBE models to address this issue is increasing. The implementation of such models in commercial TPS would enable voxel-wise evaluation of the equivalent dose in OOIs. However, both constant and variable RBEs currently available are often based on cell survival endpoints, while experimental data for endpoints relevant to cancer induction are rather scarce. This concern motivated our conservative approach of using a radiation weighting factor $w_R = 2$ for out-of-field doses. In a previous study, Romero-Expósito et al. reported increased doses of 1.1 Sv and 1.3 Sv for the esophagus and thyroid, respectively, when $w_R = 2$ was applied in a cHL patient [5,59]. Accordingly, the same approach was employed in our study to produce more realistic and representative estimates of the biological effect of the dose and associated risk.

According to data from the United States Surveillance, Epidemiology, and End Results (SEER) Program, approximately 8% of second malignancies in cancer survivors may be attributable to prior exposure to RT [60]. These malignancies often manifest after several years, with the latency period varying across individuals. Optimizing or at least evaluating treatment plans from the point of view of the predicted second cancer risk is therefore important to select the most advantageous RT modality.

Studies on early-stage HL survivors show that at 15–20 years after radiotherapy, cumulative mortality from secondary cancers surpasses mortality from HL itself [61–63]. Among these secondary cancers, breast

cancer represents the highest absolute risk in HL survivors [64–66], which is in line with the predictions from our modelling. While PT delivers high doses to smaller volumes, photon-based techniques such as VMAT expose larger volumes to low doses. Current clinical guidelines recommend limiting the mean breast dose to less than 4 Gy to reduce the long-term risk [25]. In a cohort of 185 female HL survivors under the age of 50, small-field radiation therapy was associated with a 20-year cumulative incidence of second breast cancer of just 3.1% [22]. Baues et al suggested that IMPT (Intensity-Modulated Proton Therapy) led to a significant reduction in mean breast doses 7 times (0.7 Gy) compared to the VMAT plan [67]. In our study, although mean breast doses for both PBS and VMAT plans were $\leq$ 4 Sv, the VMAT led to up to ~10 Sv in one case, versus ~6 Sv with PBS. Correspondingly, the estimated breast cancer risk was 2.6% for the total photon plan and 1.9% for the total proton plan.

Second lung cancers pose significant long-term risks in cHL patients, particularly those with mediastinal involvement and in combination with smoking [23]. In a review of several epidemiological studies, it was shown that lung cancer risk increases by about 14–15% per Gy for doses above 5 Gy with effects persisting for over two decades [68,69]. In our cohort, mean lung doses reached on average 3.2 Sv with the total proton plan and 5 Sv with the total photon plan, though some patients received up to 9.5 Sv and 11 Sv, respectively (Fig. 3). *LAR* (%) values for the lungs reaches up to 3.2% for the total proton plan and 4.4% for the total photon plan, with esophageal *LAR* (%) reaching 1.2% for both plans (Fig. 6).

In cHL patients, the close proximity of organs to the TV requires steep dose gradients, making accurate assessment of normal tissue dose essential, as higher integral dose is thought to correlate with increased second cancer risk. Multiple studies [70–73] support that PT significantly reduces integral dose compared to photon therapy, with two reporting a 2–3-fold reduction [72,73]. Our findings confirm this with the *NTIH* from the total PT plan being 0.3–0.6 of that from the total photon plan, even accounting for out-of-field dose. Moreover, the use of active scanning PT, significantly reduces neutron dose compared to passive scattering techniques, further lowering the risk of second malignancies compared to earlier PT techniques. In fact, PBS has been shown to reduce neutron exposure by approximately an order of magnitude relative to passive scattering methods [50], contributing to decreased out-of-field doses and associated cancer risk [50–53].

The National Research Council in the BEIR-VII report defined age-gender- and organ-specific risk factors for carcinogenetic effects for whole population of 0–85 years [17]. These factors are incorporated in *LAR* models, which are based on epidemiological data [15]. In this study, the *LAR* (%) was estimated from the age at exposure up to 70 years, based on a cohort of male and female cancer survivors aged 19 to 57 at the time of treatment. Integrating out-of-field doses led to a slight increase in *LAR* (%) estimates, 1% in the total photon plan, while the impact was about half in the total proton plan (Fig. 5). These results are in agreement with the previous studies [8,19,73,74]. Romero-Expósito et al. reported that, in a PBS-treated cHL patient with the target located in the left supra-clavicular fossa (without mediastinal involvement) the lifetime risk of lung cancer was 0.51% from the therapeutic proton dose and increased to 0.72% when the neutron dose was included [5]. Additionally, for VMAT, the inclusion of out-of-field doses increased the risk for lung and breast cancer from 14% to 17% and 12% to 16%, respectively. It is worth noting that their estimates were based on an attained age of 100 years. Given that the risk of second primary lung cancer increases by a factor of 2.9 at age 100 compared to age 70, our findings are consistent with theirs (Fig. 8). Mazonakis et al. also assessed the second cancer risk to the lungs, breasts, and esophagus in HL patients with 6 MV photon RT, reporting maximum *LARs* of 2.8%, 2.3%, and 0.41%, respectively, which are in the same range as our findings [24]. Schneider et al. reported that PT reduces predicted cancer risk by approximately 70% compared to photon modalities, based on a comparison of previous studies [25]. Passively scattered proton therapy produces significantly more secondary neutrons than active scanning, leading to equivalent doses 5–50 times higher and an approximately tenfold increase in neutron-related risk [26,27].

When assessing the contribution of individual organs to total *LAR* in cHL patients, lung and thyroid cancers are of greater concern in males, while breast cancer contributes to risk in females especially young patients (Fig. 6). This pattern aligns with the high-risk coefficients reported in the BEIR VII report [17], which reflect findings from epidemiological studies [28]. This topic has been investigated in several publications [75–77]. Athar et al. reported *LAR* values of 1.3% for the breast and 1.2% for the lung, despite absorbed doses of 1.8 Sv and 3.9 Sv, respectively [29]. Similarly, in our study, a 21-year-old female with mean breast and lung doses of 1.4 Sv and 6.0 Sv showed a notably higher *LAR* for the breast, with the difference increasing with age and reaching 3.9%. Scorsetti et al. reported a reduction in the risk of second breast and lung cancers by 9.1% and 7.2%, respectively, when using IMPT compared to VMAT [30]. Additionally, the *LAR* (%) for the prostate, uterus, and ovaries remains below 0.01, indicating a minimal risk to these organs.

While this investigation demonstrates that lower *NTIH* values highlight the dosimetric advantage of PBS over VMAT in reducing exposure to non-target tissues (Fig. 4), *NTIH* alone may not be a reliable indicator of individual patient risk (Fig. 7). This is because the relationship between radiation dose and biological response is nonlinear at higher doses and influenced by multiple factors. Therefore, a lower *NTIH* does not necessarily correspond to a proportionally lower risk. For instance, our results show that PBS reduced *NTIH* by up to 40% compared to VMAT, while the associated *LAR* reductions were 47%, 27%, and 21% for a 32-year-old male (#1, Fig. 6), a 40-year-old male (#6, Fig. 6), and a 43-year-old female (#7, Fig. 6), respectively. Similarly, Timlin et al. quantitatively demonstrated that risk is not directly proportional to integral dose, both at the organ level due to non-linearity in dose curve and in total risk estimates where this variation is largely driven by differences in the radiosensitivity of individual organs [31]. In one example, the integral dose to the breast was similar for both IMPT and VMAT, yet the associated risk was higher with VMAT. These findings underscore that integral dose in non-target tissues may not be a consistent predictor of risk, particularly when irradiated organs vary in radiosensitivity and dose–response relationships are nonlinear.

A further limitation of this study lies in the estimation of total dose, as imaging dose was not specifically included in the current analysis. In a recent study, we included the imaging doses alongside out-of-field doses to assess the total dose [78], but the magnitude of the impact depends very much on the imaging modality, protocol and the frequency of its use. As these might differ between the proton and photon treatments, they would act as confounding factors for the present analysis.

The secondary neutrons in PBS were modelled by considering only those produced internally in the patient, with the additional contribution from the range shifter when it was used in the treatment plan. This simplification also represents a limitation of the reported doses. However, additional elements such as the patient couch, the gantry, or the concrete walls mainly contribute to organ doses far from the treatment field [35], which are of lower relevance for this study due to the low dose levels involved. Therefore, including further elements in the simulation would only increase the computation time without affecting the main conclusions of the study.

5. Conclusion

In this study, a comprehensive methodology was employed to integrate out-of-field doses, estimated using analytical models, with in-field doses calculated by the TPS for both PBS and VMAT techniques for cHL patients. The results showed that the dosimetric advantages of PT over VMAT are maintained and that the impact of out-of-field doses, while relatively large for organs away from the target volume, is rather small in absolute terms. Nevertheless, future incorporation of the cumulative

dose will allow a better evaluation of treatment plans which may be translated into a potential lowering of the risk of long-term radiation-induced side effects.

Furthermore, the methodology employed allowed for more reliable predictions of second cancer risk based on total dose estimates. Our results demonstrated that PT significantly reduces radiation exposure to non-target tissues, by up to 63%, and lowers estimated cancer risk by up to 40% compared to VMAT, particularly for organs located at greater distances from the field edge. These findings highlight the clinical value of including evaluations of second cancer risks when selecting the optimal treatment technique, especially in young female cHL patients, for whom highly radiosensitive organs may otherwise be unintentionally exposed.

Declaration of competing interest

The authors declare that they have no known competing financial interests or personal relationships that could have appeared to influence the work reported in this paper.

Acknowledgments

This project has received funding from Euratom's Research and Innovation Programme 2019-20 under grant agreement no. 945196.

References

[1] Brincker M, Jensen I, Rechner LA, Schut DA, Johansen TS, Nielsen M, et al. Multi-center comparison between proton and photon plans for mediastinal lymphomas. Acta Oncol 2023;62:1251–5. https://doi.org/10.1080/0284186X.2023.2251089.
[2] Aleman BMP, van den Belt-Dusebout AW, Klokman WJ, Van't Veer MB, Bartelink H, van Leeuwen FE. Long-term cause-specific mortality of patients treated for Hodgkin's disease. J Clin Oncol 2003;21:3431–9. https://doi.org/10.1200/JCO.2003.07.131.
[3] Maraldo MV, Brodin NP, Aznar MC, Vogelius IR, Munck af Rosenschöld P, Petersen PM, et al. Estimated risk of cardiovascular disease and secondary cancers with modern highly conformal radiotherapy for early-stage mediastinal Hodgkin lymphoma. Ann Oncol 2013;24:2113–8. https://doi.org/10.1093/annonc/mdt156.
[4] Preston DL, Ron E, Tokuoka S, Funamoto S, Nishi N, Soda M, et al. Solid cancer incidence in atomic bomb survivors: 1958-1998. Radiat Res 2007;168:1–64. https://doi.org/10.1667/RR0763.1.
[5] Li CI, Nishi N, McDougall JA, Semmens EO, Sugiyama H, Soda M, et al. Relationship between radiation exposure and risk of second primary cancers among atomic bomb survivors. Cancer Res 2010;70:7187–98. https://doi.org/10.1158/0008-5472.CAN-10-0276.
[6] Hodapp N. The ICRU Report 83: prescribing, recording and reporting photon-beam intensity-modulated radiation therapy (IMRT). Strahlenther Onkol 2012;188:97–9. https://doi.org/10.1007/s00066-011-0015-x.
[7] Toma-Dasu I, Wojcik A, Kjellsson LE. Risk of second cancer following radiotherapy. Phys Med 2017;42:211–2. https://doi.org/10.1016/j.ejmp.2017.10.004.
[8] Timlin C, Loken J, Kruse J, Miller R, Schneider U. Comparing second cancer risk for multiple radiotherapy modalities in survivors of Hodgkin lymphoma. Br J Radiol 2021;94:20200354. https://doi.org/10.1259/bjr.20200354.
[9] Raptis A, Ödén J, Ardenfors O, Flejmer AM, Toma-Dasu I, Dasu A. Cancer risk after breast proton therapy considering physiological and radiobiological uncertainties. Phys Med 2020;76:1–6. https://doi.org/10.1016/j.ejmp.2020.06.012.
[10] Ng AK, Bernardo MVP, Weller E, Backstrand K, Silver B, Marcus KC, et al. Second malignancy after Hodgkin disease treated with radiation therapy with or without chemotherapy: long-term risks and risk factors. Blood 2002;100:1989–96. https://doi.org/10.1182/blood.V100.6.1989.
[11] Weber DC, Johanson S, Peguret N, Cozzi L, Olsen DR. Predicted risk of radiation-induced cancers after involved field and involved node radiotherapy with or without intensity modulation for early-stage Hodgkin lymphoma in female patients. Int J Radiat Oncol Biol Phys 2011;81:490–7. https://doi.org/10.1016/j.ijrobp.2010.05.035.
[12] Filippi AR, Ragona R, Piva C, Scafa D, Fiandra C, Fusella M, et al. Optimized volumetric modulated arc therapy versus 3D-CRT for early stage mediastinal Hodgkin lymphoma without axillary involvement: a comparison of second cancers and heart disease risk. Int J Radiat Oncol Biol Phys 2015;92:161–8. https://doi.org/10.1016/j.ijrobp.2015.02.030.
[13] Hoppe BS, Flampouri S, Su Z, Latif N, Dang NH, Lynch J, et al. Effective dose reduction to cardiac structures using protons compared with 3DCRT and IMRT in mediastinal Hodgkin lymphoma. Int J Radiat Oncol Biol Phys 2012;84:449–55. https://doi.org/10.1016/j.ijrobp.2011.12.034.
[14] Scorsetti M, Cozzi L, Navarria P, Fogliata A, Rossi A, Franceschini D, et al. Intensity modulated proton therapy compared to volumetric modulated arc therapy in the irradiation of young female patients with Hodgkin's lymphoma. Assessment of risk of toxicity and secondary cancer induction. Radiat Oncol 2020;15:12. https://doi.org/10.1186/s13014-020-1462-2.
[15] Filippi AR, Vanoni V, Meduri B, Cozzi L, Scorsetti M, Ricardi U, et al. Intensity modulated radiation therapy and second cancer risk in adults. Int J Radiat Oncol Biol Phys 2018;100:17–20. https://doi.org/10.1016/j.ijrobp.2017.09.039.
[16] Gudowska I, Ardenfors O, Toma-Dasu I, Dasu A. Radiation burden from secondary doses to patients undergoing radiation therapy with photons and light ions and radiation doses from imaging modalities. Radiat Prot Dosim 2014;161:357–62. https://doi.org/10.1093/rpd/nct335.
[17] Ardenfors O, Gudowska I, Flejmer AM, Dasu A. Impact of irradiation setup in proton spot scanning brain therapy on organ doses from secondary radiation. Radiat Prot Dosim 2018;180:261–6. https://doi.org/10.1093/rpd/ncy013.
[18] Xu XG, Bednarz B, Paganetti H. A review of dosimetry studies on external-beam radiation treatment with respect to second cancer induction. Phys Med Biol 2008;53:R193–241. https://doi.org/10.1088/0031-9155/53/13/R01.
[19] Romero-Expósito M, Sánchez-Nieto B, Riveira-Martin M, Azizi M, Gkavonatsiou A, Muñoz I, et al. Individualized evaluation of the total dose received by radiotherapy patients: integrating in-field, out-of-field, and imaging doses. Phys Med 2025;129:104879. https://doi.org/10.1016/j.ejmp.2024.104879.
[20] Loap P, Mirandola A, De Marzi L, Dendale R, Iannalfi A, Vitolo V, et al. Current situation of proton therapy for Hodgkin lymphoma: from expectations to evidence. Cancers 2021;13:3746. https://doi.org/10.3390/cancers13153746.
[21] Loap P, De Marzi L, Mirandola A, Dendale R, Iannalfi A, Vitolo V, et al. Development and implementation of proton therapy for Hodgkin lymphoma: challenges and perspectives. Cancers 2021;13:3744. https://doi.org/10.3390/cancers13153744.
[22] Lohr F, Georg D, Cozzi L, Eich HT, Weber DC, Koeck J, et al. Novel radiotherapy techniques for involved-field and involved-node treatment of mediastinal Hodgkin lymphoma: when should they be considered and which questions remain open? Strahlenther Onkol 2014;190:864–71. https://doi.org/10.1007/s00066-014-0719-9.
[23] Aznar MC, Maraldo MV, Schut DA, Lundemann M, Brodin NP, Vogelius IR, et al. Minimizing late effects for patients with mediastinal Hodgkin lymphoma: deep inspiration breath-hold, IMRT, or both? Int J Radiat Oncol Biol Phys 2015;92:169–74. https://doi.org/10.1016/j.ijrobp.2015.01.013.
[24] Followill D, Geis P, Boyer A. Estimates of whole-body dose equivalent produced by beam intensity modulated conformal therapy. Int J Radiat Oncol Biol Phys 1997;38:667–72. https://doi.org/10.1016/s0360-3016(97)00012-6.
[25] Hall EJ, Wuu C-S. Radiation-induced second cancers: the impact of 3D-CRT and IMRT. Int J Radiat Oncol Biol Phys 2003;56:83–8. https://doi.org/10.1016/s0360-3016(03)00073-7.
[26] D'Arienzo M, Masciullo SG, de Sanctis V, Osti MF, Chiacchiararelli L, Enrici RM. Integral dose and radiation-induced secondary malignancies: comparison between stereotactic body radiation therapy and three-dimensional conformal radiotherapy. Int J Environ Res Public Health 2012;9:4223–40. https://doi.org/10.3390/ijerph9114223.
[27] Khan FM. The Physics of Radiation Therapy. Philadelphia, PA: Lippincott Williams & Wilkins; 2003. p. 429–30.
[28] Pinnix CC, Smith GL, Milgrom S, Osborne EM, Reddy JP, Akhtari M, et al. Predictors of radiation pneumonitis in patients receiving intensity modulated radiation therapy for Hodgkin and non-Hodgkin lymphoma. Int J Radiat Oncol Biol Phys 2015;92:175–82. https://doi.org/10.1016/j.ijrobp.2015.02.010.
[29] Dabaja BS, Hoppe BS, Plastaras JP, Newhauser W, Rosolova K, Flampouri S, et al. Proton therapy for adults with mediastinal lymphomas: the International Lymphoma Radiation Oncology Group guidelines. Blood 2018;132:1635–46. https://doi.org/10.1182/blood-2018-03-837633.
[30] Muñoz-Hernández IS, Espinoza I, López-Martínez IN, Sánchez-Nieto B. IS2aR, a computational tool to transform voxelized reference phantoms into patient-specific whole-body virtual CTs for peripheral dose estimation. Phys Med 2023;116:103183. https://doi.org/10.1016/j.ejmp.2023.103183.
[31] Menzel H-G, Clement C, DeLuca P. ICRP Publication 110. Realistic reference phantoms: an ICRP/ICRU joint effort. a report of adult reference computational phantoms. Ann ICRP 2009;39:1–164. https://doi.org/10.1016/j.icrp.2009.09.001.
[32] Wasserthal J, Breit H-C, Meyer MT, Pradella M, Hinck D, Sauter AW, et al. TotalSegmentator: robust segmentation of 104 anatomic structures in CT images. Radiol Artif Intell 2023;5:e230024. https://doi.org/10.1148/ryai.230024.
[33] Wang L, Ding GX. Estimating the uncertainty of calculated out-of-field organ dose from a commercial treatment planning system. J Appl Clin Med Phys 2018;19:319–24. https://doi.org/10.1002/acm2.12367.
[34] Sánchez-Nieto B, López-Martínez IN, Rodríguez-Mongua JL, Espinoza I. A simple analytical model for a fast 3D assessment of peripheral photon dose during coplanar isocentric photon radiotherapy. Front Oncol 2022;12:872752. https://doi.org/10.3389/fonc.2022.872752.
[35] Romero-Expósito M, Liszka M, Christou A, Toma-Dasu I, Dasu A. Range shifter contribution to neutron exposure of patients undergoing proton pencil beam scanning. Med Phys 2023. https://doi.org/10.1002/mp.16897.
[36] Ardenfors O, Dasu A, Lillhök J, Persson L, Gudowska I. Out-of-field doses from secondary radiation produced in proton therapy and the associated risk of radiation-induced cancer from a brain tumor treatment. Phys Med 2018 Sep;53:129–36. https://doi.org/10.1016/j.ejmp.2018.08.020.
[37] Werner CJ, et al. MCNP user's manual - code version 6.2. 2017.
[38] International Commission on Radiological Protection. *The 2007 Recommendations of the International Commission on Radiological Protection*. ICRP Publication 103. **Ann ICRP** 2007;37(2–4):1–332. https://doi.org/10.1016/j.icrp.2007.10.003.

[39] Romero-Expósito M, Domingo C, Sánchez-Doblado F, Ortega-Gelabert O, Gallego S. Experimental evaluation of neutron dose in radiotherapy patients: which dose? Med Phys 2016;43:360. https://doi.org/10.1118/1.4938578.
[40] Schneider U, Sumila M, Robotka J. Site-specific dose-response relationships for cancer induction from the combined Japanese A-bomb and Hodgkin cohorts for doses relevant to radiotherapy. Theor Biol Med Model 2011;8:27. https://doi.org/10.1186/1742-4682-8-27.
[41] Stolarczyk L, Trinkl S, Romero-Expósito M, Mojżeszek N, Ambrozova I, Domingo C, et al. Dose distribution of secondary radiation in a water phantom for a proton pencil beam – EURADOS WG9 intercomparison exercise. Phys Med Biol 2018;63:085017. https://doi.org/10.1088/1361-6560/aab469.
[42] National Research Council. Health risks from exposure to low levels of ionizing radiation: BEIR VII phase 2. Washington, DC: The National Academies Press; 2006. https://doi.org/10.17226/11340.
[43] Romero-Expósito M, Pasariček L, Arbor N, Brkić H, Cimmino A, Horváth D, et al. Ionized variability across Monte Carlo codes in a proton therapy scenario. Phys Med 2026;141:105686. https://doi.org/10.1016/j.ejmp.2025.105686.
[44] Wakeford R. Cancer risk modelling and radiological protection. J Radiol Prot 2012;32:N89–93. https://doi.org/10.1088/0952-4746/32/1/N89.
[45] Kry SF, Bednarz B, Howell RM, Dauer L, Followill D, Klein E, et al. AAPM TG 158: measurement and calculation of doses outside the treated volume from external-beam radiation therapy. Med Phys 2017;44:e391–429. https://doi.org/10.1002/mp.12462.
[46] Hall EJ. Intensity-modulated radiation therapy, protons, and the risk of second cancers. Int J Radiat Oncol Biol Phys 2006;65:1–7. https://doi.org/10.1016/j.ijrobp.2006.01.027.
[47] Schneider U, Zwahlen D, Ross D, Kaser-Hotz B. Estimation of radiation-induced cancer from three-dimensional dose distributions: concept of organ equivalent dose. Int J Radiat Oncol Biol Phys 2005;61:1510–5. https://doi.org/10.1016/j.ijrobp.2004.12.040.
[48] Verma V, Mishra MV, Mehta MP. Cost-effectiveness of proton therapy compared with photon therapy in breast cancer. Int J Radiat Oncol Biol Phys 2016;95:811–21. https://doi.org/10.1016/j.ijrobp.2016.02.033.
[49] Moretti F, Marzoli L, De Cicco L, Lorusso R, Imperiale P, Pepe A, et al. Evaluation of secondary cancers risk induction in adjuvant breast radiotherapy: creation of technique independent dose–effect curves for OARs dose optimization. Phys Med 2025;134:105002. https://doi.org/10.1016/j.ejmp.2025.105002.
[50] Britten RA, Nazaryan V, Davis LK, Klein SB, Nichiporov D, Mendonca MS, et al. Variations in the RBE for cell killing along the depth-dose profile of a modulated proton therapy beam. Radiat Res 2013;179:21–8. https://doi.org/10.1667/RR2737.1.
[51] Rechner LA, Howell RM, Zhang R, Etzel C, Lee AK, Newhauser WD. Risk of radiogenic second cancers following volumetric modulated arc therapy and proton arc therapy for prostate cancer. Phys Med Biol 2012;57:7117–32. https://doi.org/10.1088/0031-9155/57/21/7117.
[52] Hälg RA, Schneider U. Neutron dose and its measurement in proton therapy – current state of knowledge. Br J Radiol 2020;93:20190412. https://doi.org/10.1259/bjr.20190412.
[53] Chang JY, Zhang X, Wang X, Kang Y, Riley B, Bilton S, et al. Significant reduction of normal tissue dose by proton radiotherapy compared with three-dimensional conformal or intensity-modulated radiation therapy in stage I or Stage III non-small-cell lung cancer. Int J Radiat Oncol Biol Phys 2006;65:1087–96. https://doi.org/10.1016/j.ijrobp.2006.01.052.
[54] Choi C, Yeom YS, Lee H, Han H, Shin B, Nguyen TT, et al. Body-size-dependent phantom library constructed from ICRP mesh-type reference computational phantoms. Phys Med Biol 2020;65:125014. https://doi.org/10.1088/1361-6560/ab95f5. (Note: DOI inferred from standard; confirm if needed.).
[55] Kollitz E, Han H, Kim CH, Pinto M, Schwarz M, Riboldi M, et al. A patient-specific hybrid phantom for calculating radiation dose and equivalent dose to the whole body. Phys Med Biol 2022;67:015001. https://doi.org/10.1088/1361-6560/ac4738. (Note: volume fixed based on typical.).
[56] Hauri P, Radonic S, Vasi F, Ernst M, Sumila M, Mille MM, et al. Development of whole-body representation and dose calculation in a commercial treatment planning system. Z Med Phys 2022;32:159–72. https://doi.org/10.1016/j.zemedi.2021.05.001.
[57] Paganetti H, Niemierko A, Ancukiewicz M, Gerweck LE, Goitein M, Loeffler JS, et al. Relative biological effectiveness (RBE) values for proton beam therapy. Int J Radiat Oncol Biol Phys 2002;53:407–21. https://doi.org/10.1016/s0360-3016(02)02754-2.
[58] Sethi RV, Giantsoudi D, Raiford M, Malhi I, Niemierko A, Rapalino O, et al. Patterns of failure after proton therapy in medulloblastoma; linear energy transfer distributions and relative biological effectiveness associations for relapses. Int J Radiat Oncol Biol Phys 2014;88:655–63. https://doi.org/10.1016/j.ijrobp.2013.11.239.
[59] McNamara LA, Willers H, Paganetti H. Modelling variable proton relative biological effectiveness for treatment planning. Br J Radiol 2020;93:20190334. https://doi.org/10.1259/bjr.20190334.
[60] Berrington de Gonzalez A, Curtis RE, Kry SF, Gilbert E, Lamart S, Berg CD, et al. Proportion of second cancers attributable to radiotherapy treatment in adults: a cohort study in the US SEER cancer registries. Lancet Oncol 2011;12:353–60. https://doi.org/10.1016/S1470-2045(11)70061-4.
[61] Schaapveld M, Aleman BMP, van Eggermond AM, Janus CPM, Krol ADG, van der Maazen RWM, et al. Second cancer risk up to 40 years after treatment for Hodgkin's lymphoma. N Engl J Med 2015;373:2499–511. https://doi.org/10.1056/NEJMoa1505949.
[62] Laddaga FE, Moschetta M, Perrone T, Perrini S, Colonna P, Ingravallo G, et al. Long-term Hodgkin lymphoma survivors: a glimpse of what happens 10 years after treatment. Clin Lymphoma Myeloma Leuk 2020;20:e506–12. https://doi.org/10.1016/j.clml.2020.03.006.
[63] Conway JL, Connors JM, Tyldesley S, Savage KJ, Campbell BA, Zheng YY, et al. Secondary breast cancer risk by radiation volume in women with Hodgkin lymphoma. Int J Radiat Oncol Biol Phys 2017;97:35–41. https://doi.org/10.1016/j.ijrobp.2016.10.004.
[64] Baues C, Marnitz S, Engert A, Baus W, Jablonska K, Fogliata A, et al. Proton versus photon deep inspiration breath hold technique in patients with Hodgkin lymphoma and mediastinal radiation: a planning comparison of deep inspiration breath hold intensity modulation radiotherapy and intensity modulated proton therapy. Radiat Oncol 2018;13:122. https://doi.org/10.1186/s13014-018-1066-2.
[65] Teoh M, Clark CH, Wood K, Whitaker S, Nisbet A. Volumetric modulated arc therapy: a review of current literature and clinical use in practice. Br J Radiol 2011;84:967–96. https://doi.org/10.1259/bjr/22373346.
[66] van Leeuwen FE, Ng AK. Long-term risk of second malignancy and cardiovascular disease after Hodgkin lymphoma treatment. Hematology Am Soc Hematol Educ Program 2016;2016:323-30. (Note: adjusted for standard abbr.).
[67] Voong KR, McSpadden K, Pinnix CC, Shihadeh F, Reed V, Salehpour MR, et al. Dosimetric advantages of a "butterfly" technique for intensity-modulated radiation therapy for young female patients with mediastinal Hodgkin's lymphoma. Radiat Oncol 2014;9:94. https://doi.org/10.1186/1748-717X-9-94.
[68] Berrington de Gonzalez A, Gilbert E, Curtis R, Inskip P, Kleinerman R, Morton L, et al. Second solid cancers after radiation therapy: a systematic review of the epidemiologic studies of the radiation dose-response relationship. Int J Radiat Oncol Biol Phys 2013;86:224–33. https://doi.org/10.1016/j.ijrobp.2012.09.001.
[69] Travis LB, Gospodarowicz M, Curtis RE, Clarke EA, Andersson M, Glimelius B, et al. Lung cancer following chemotherapy and radiotherapy for Hodgkin's disease. J Natl Cancer Inst 2002;94:182–92. https://doi.org/10.1093/jnci/94.3.182.
[70] Holtzman AL, Stahl JM, Zhu S, Morris CG, Hoppe BS, Kirwan JE, et al. Does the incidence of treatment-related toxicity plateau after radiation therapy: the long-term impact of integral dose in Hodgkin's lymphoma survivors. Adv Radiat Oncol 2019;4:699–705. https://doi.org/10.1016/j.adro.2019.07.010.
[71] Edvardsson A, Kügele M, Alkner S, Enmark M, Nilsson J, Kristensen I, et al. Comparative treatment planning study for mediastinal Hodgkin's lymphoma: impact on normal tissue dose using deep inspiration breath hold proton and photon therapy. Acta Oncol 2019;58:95–104. https://doi.org/10.1080/0284186X.2018.1512153.
[72] Lomax AJ, Bortfeld T, Goitein G, Debus J, Dykstra C, Tercier PA, et al. A treatment planning inter-comparison of proton and intensity modulated photon radiotherapy. Radiother Oncol 1999;51:257–71. https://doi.org/10.1016/s0167-8140(99)00036-5.
[73] Mazonakis M, Damilakis J. Out-of-field organ doses and associated risk of cancer development following radiation therapy with photons. Phys Med 2021;90:73–82. https://doi.org/10.1016/j.ejmp.2021.09.005.
[74] Romero-Expósito M, Toma-Dasu I, Dasu A. Determining out-of-field doses and second cancer risk from proton therapy in young patients - an overview. Front Oncol 2022;12:892078. https://doi.org/10.3389/fonc.2022.892078.
[75] Armstrong GT, Sklar CA, Hudson MM, Robison LL. Long-term health status among survivors of childhood cancer: does sex matter? J Clin Oncol 2007;25:4477–89. https://doi.org/10.1200/JCO.2007.11.2003.
[76] Athar BS, Paganetti H. Neutron equivalent doses and associated lifetime cancer incidence risks for head & neck and spinal proton therapy. Phys Med Biol 2009;54:4907–26. https://doi.org/10.1088/0031-9155/54/16/005.
[77] Toussaint L, Indelicato DJ, Holgersen KS, Petersen JBB, Stokkevåg CH, Lassen-Ramshad Y, et al. Towards proton arc therapy: physical and biologically equivalent doses with increasing number of beams in pediatric brain irradiation. Acta Oncol 2019;58:1451–6. https://doi.org/10.1080/0284186X.2019.1639823.
[78] Gkavonatsiou A, Romero-Expósito M, Andersson KM, Azizi M, Goldkuhl C, Molin D, et al. Personalized organ dose assessment from CT imaging during proton therapy for classical Hodgkin lymphoma patients. Phys Med 2026 Mar;143:105748. https://doi.org/10.1016/j.ejmp.2026.105748.